Diagnostics at high repetition rates: new insights into transient combustion phenomena

B. Böhm, C. Kittler, A. Nauert, A. Dreizler*

FG Energie- und Kraftwerkstechnik, TU Darmstadt, Petersenstr. 30, D-64287 Darmstadt

Abstract

This contribution highlights recent advances in laser diagnostics at high repetition rates. Based on recent improvements in all-solid-state diode-pumped laser- and CMOS camera-technology well known methods such as chemiluminescence, Mie scattering or planar laser-induced fluorescence are adapted and extended to high repetition rates in the kHz-regime. These high repetition rates enable to track transient events in turbulent combustion such as flame extinction or flash back temporally. New perspectives into turbulent combustion are thus possible by conditioning on transient phenomena or quasi-4D imaging.

Introduction

Laser diagnostics play a vital role to gain a deeper insight into complex chemical and physical processes in turbulent flames. So far, statistically uncorrelated information was sampled by repetition rates of typically few 10 Hz. This allowed to measure probability density functions of various scalar and vectorial quantities such as temperature, species concentrations, mixture fraction, scalar dissipation rate, fluid velocities, Reynolds-stress components, vorticity or dilatation. For statistically stationary combustion processes these diagnostics helped significantly for an improved understanding of non-premixed and premixed flames. However, in some practical applications turbulent flames are prone to instabilities such as flame extinction or flashback. As these phenomena are transient in nature and unpredictable in their onset, advanced diagnostic tools are required to temporally resolve such processes.

Recent improvements of diode-pumped solid-state lasers and CMOS camera technology allow the application of various well-established diagnostics such as Mie scattering [1], particle imaging velocimetry [2,3] or laser-induced fluorescence [4,5] at repetition rates in the kHz-regime. Thereby temporal resolution below typical integral time-scales of turbulent flames is accessible. This allows tracking the evolution of transient phenomena such as flame extinction, ignition [6,7], flame stabilization or flashback temporally.

The present contribution highlights recent advances of diagnostics at repetition rates up to 30 kHz. Examples of applications are turbulent mixing, flame extinction in a partially-premixed turbulent opposed jet burner and flashback in a premixed swirl-flame. Preliminary OH planar laser-induced fluorescence (PLIF) measurements are presented to show the feasibility of planar flame-radical detection at 5 kHz.

Experimental

Different types of lasers were used in the present study. For repetition rates up to 30 kHz a conventional argon-ion laser (Coherent Innova) was used. The power was limited to 2.5 W. Thereby this laser was suitable only for Mie scattering from aerosol particles that can be used to visualize mixing processes (Quantitative Light Scattering, see [8]) or for particle imaging velocimetry (PIV) [9]. Simultaneous chemi-luminescence and Mie scattering for the visualization of turbulence–chemistry interactions were performed using a pulsed all-solid-state laser (Nd:YLF Evolution 90, Coherent). To some extent the Mie scattering (without simultaneous chemiluminescence measurements) was used additionally for high-speed PIV evaluations during the instant of flame extinction. For these experiments a different solid-state laser was used that was more flexible in generating double-pulses (Nd:YVO_4 EdgeWave, IS4II-DE).

For planar laser-induced fluorescence (PLIF) of radicals relevant to combustion processes such as hydroxyl (OH), tunable radiation in the ultraviolet spectral range is required. For this purpose an intra-cavity frequency-doubled diode-pumped all-solid-state Nd:YLF laser (Coherent Evolution 90) was operated at 5 kHz repetition rate to pump a tunable dye laser. The average power of the pump laser peaked up to 90 W. This corresponded to single-pulse energies of 18 mJ. The pulse length was 170 ns limiting the overall conversion efficiency of UV-generation in the dye laser. The dye laser was based on a conventional system designed originally for 10 Hz operation (Radiant Dyes). To adapt the dye laser to the needs of high repetition rates, several modifications of the laser were essential. The low pump energies allowed pumping only the oscillator and the preamplifier. Consequently no main amplifier was operated. The dye cuvette was connected to a dye circulator equipped with a stronger pump than in 10 Hz-applications and a larger dye reservoir. Flow rates of the dye were 12 l/min. The delay-line of the beam pumping the preamplifier was shortened to minimize the losses due to the relatively large divergence of the pump laser. To optimize the conversion rate of the fundamental wavelength from 566 nm to 283 nm, a 25 mm long frequency-doubling (BBO) crystal was used. By this means the conversion efficiency was enhanced significantly compared to the conventional crystal in the 10 Hz-applications. A general issue was the long-term stability. To reduce

* Corresponding author: dreizler@ekt.tu-darmstadt.de

thermal drifts, the rear panel of the cuvette mount was water-cooled. The output coupling mirror was shielded by masks from both sides to prevent heating of the mount by radiation other than the laser beam. The maximum average output power achieved at 283 nm was 180 mW. This corresponds to pulse energies of 36 µJ. However, the average power dropped after alignment due to remaining thermal drifts over a period of several minutes. This clearly indicates that further improvements of the long-term stability are essential. The spectral width was approximately 0.04 cm^{-1} based on etalon measurements.

Signals from chemiluminescence (CL), Mie scattering and fluorescence, respectively, were monitored by a state-of-the art CMOS camera (LaVision, HSS5). At maximal repetition rates of 30 kHz the exposure time was 10 µs. At this high repetition rates 256 x 256 pixels of the CMOS were active. At 10 kHz the usable area of the array increased to 512 x 512 pixels. The A/D-conversion had a dynamic range of 10 bit. If not stated otherwise the CMOS camera was equipped with a lens-coupled two-stage image intensifier (High Speed IRO, LaVision). In case of 5 kHz PLIF the gate width of the IRO was set to 500 ns. For Mie and CL measurements the gate width was in the order of few µs.

Two flow configurations were investigated, namely a turbulent opposed jet and a swirling flow. In the turbulent opposed jet configuration [10], shown at the left hand side of figure 1, the non-reacting mixing layer was investigated by Mie scattering of aerosol particles. Aerosol was seeded hereby only to the lower fluid flow. In case of reacting conditions CL and Mie were measured simultaneously during extinction of a partially-premixed flame. In this case both flows were seeded. The fuel was composed of 17.4 vol% CH_4 in air. The Reynolds-numbers were 7200 corresponding to flames at the extinction limit [10].

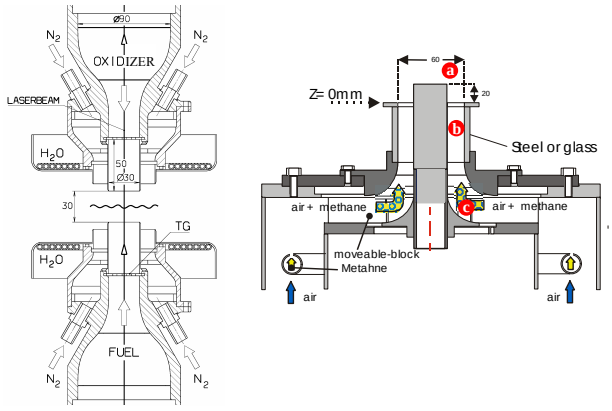

Figure 1: Sketch of the turbulent opposed jet configuration (left) and the swirling nozzle (right) with its swirl-dependent stabilization points (a, b, c).

Figure 2 shows the optical layout of the Mie experiment using the argon-ion laser. The laser beam was formed to a light sheet 20 mm in height and 1 mm wide. The beam was scanned across the probe volume by a galvanic mirror (GSI Lumonics). The maximum scan rate per sweep was 2 kHz. Multiple 2D planes were monitored successively over a range of 15 mm. The depth of field of the camera lens was adapted to this range. The field of view in this case was 12 x 12 mm. In case of the simultaneous CL and Mie experiments the argon-ion laser was replaced by the pulsed all-solid-state laser as mentioned above.

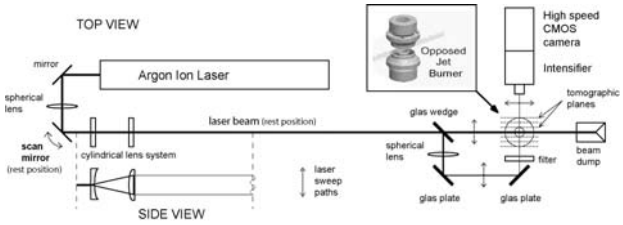

Figure 2: Optical setup for Mie scattering experiments in the opposed jet configuration.

The swirling nozzle is shown at the right hand side of figure 1. It is based on a design presented in [11,12]. A central 30 mm-diameter bluff-body is surrounded by a 15 mm wide annular slot. The central bluff-body sticks out by 20 mm. By this means the transition from stable flames to flashback could be controlled (see below). The outer tube of the nozzle was build originally from steel. It was replaced by a quartz tube to enable optical access during flashback. The moveable block design allowed to change the theoretical swirl number from 0 to 2. The swirl number S was changed automatically by rotating the moveable block with a stepper motor. Minimal increments were $\Delta S = 0.02$. For $S<0.8$ the flame was stable (see Fig. 1, a). At $S \geq 0.8$ the flame passed over into a metastable state. It started to spin around the bluff-body while the stabilization point moved from above the bluff-body to its top and further upstream along its shell (b). Passing $S=1.0$ the flame flashed back into the swirler (c). Figure 3 shows snap-shots of the CL for different swirl numbers taken with the CMOS camera at a repetition rate of 7.2 kHz.

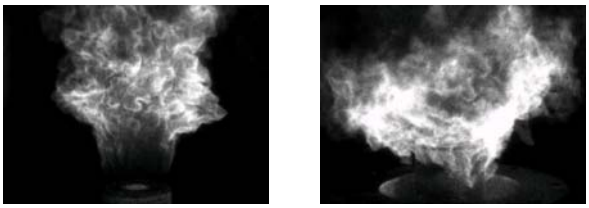

Figure 3: Snap-shots of the turbulent premixed flame at different swirl numbers. For $S=0$, the flame stabilizes at the top of the bluff-body (left) and for $S=0.8$ it starts to spin around the bluff-body and moves upstream (right).

With the OH PLIF experiments at a repetition rate of 5 kHz new ground is broken. So far OH PLIF measurements were restricted to 1 kHz [4] to the best of the authors´ knowledge. The dye laser was tuned to the $Q_1 6$ line in the $A^2\Sigma$-$X^2\Pi$ (1-0) band. The laser sheet height was approximately 15 mm. OH radicals were

monitored in the flame shown in the left part of figure 3. The aim was to visualize the temporal variation of the OH radical distribution. For this feasibility study the signals were not corrected for pulse-to-pulse fluctuations of the total energy or variations in the laser profile.

Results and discussions

Mie scattering at 30 kHz

In non- and partially-premixed flames reaction takes place within the mixing layer of fuel and oxidizer. It is therefore of special interest to visualize and understand the dynamics of turbulent mixing layers. A generic bench mark for such investigations is the turbulent opposed jet configuration.

The turbulent non-reacting mixing layer in the turbulent opposed jet configuration, shown at the left hand side of figure 1, was investigated by Mie scattering where only the lower flow was seeded by aerosols. Figure 4 shows an example of a sweep of the laser beam across ±7.5 mm around the symmetry axis of the burner. The repetition rate of the CMOS camera was 30 kHz with an exposure time of 10 µs. The clearance between the 15 measurement planes varies according to the sinusoidal motion of the scanning mirror. The duration of the complete sweep was 500 µs, well below large eddy turn over times in the order of 16 ms [10,13]. Thereby the instantaneous eddy appears frozen during the sweep. From this tomographic 2D-information the topology of the mixing surface between both flows can be reconstructed in quasi-3D.

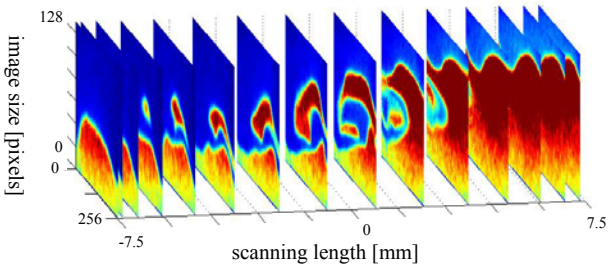

Figure 4: Mie scattering from aerosols shown in false colors. These 15 planes have been recorded consecutively during 500 µs (30 kHz).

As the sweeps were repeated temporally at 2 kHz, one can monitor the temporal evolution of the mixing layer. For this purpose, 2D-images as in figure 4 were converted to binary images. Using 15 binary images from a single sweep, the quasi-instantaneous 2D-interface between upper and lower fluid flow was reconstructed by a triangulation procedure [14]. Figure 5 shows the temporal evolution of the mixing layer. In this figure only every 3rd sweep is shown (1.5 ms between images). This shows the feasibility for quasi-4D diagnostics using repetition rates in the kHz-regime.

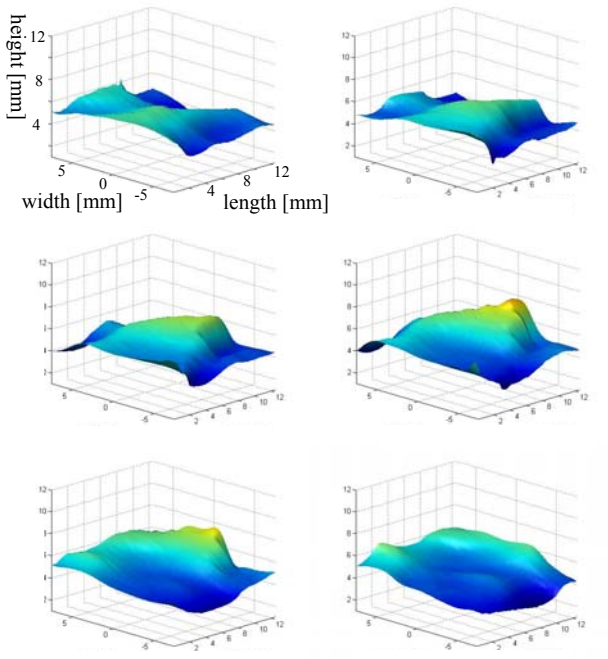

Figure 5: Each of the six images shows an instantaneous mixing layer reconstructed from tomographic 2D Mie scattering images during one sweep as shown in figure 4.

Simultaneous Mie scattering and chemiluminescence

Under chemically reacting conditions Mie scattering can be combined with chemiluminescence. Whereas the particles observed by Mie scattering represent the turbulent fluid motion in a two-dimensional plane, chemiluminescence gives an estimation of the approximate flame position.

In the example shown in figure 6 the CMOS camera (without IRO) was operated at 1 kHz while Mie scattering of 0.5 µm MgO particles was laser-excited at 10 kHz. Each exposure shows particle trajectories of up to 10 subsequent particle positions on top of the

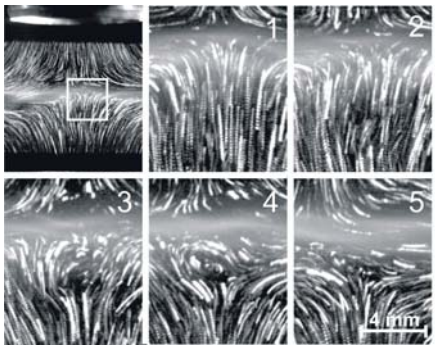

Figure 6: Simultaneously measured flame luminosity (grey areas) and Mie scattering from 10 laser shots during each 1kHz camera exposure. Temporal sequence (images 1-5) are from the 11.5x11.5mm^2 white box in the left top image.

chemiluminescence image. In the selected example the formation of an eddy is highlighted. The formation of such eddies generate vorticity when the fluid approaches the turbulent flame located in the vicinity of the mean stagnation plane [15].

High speed PIV conditioned on extinction

Instead of using chemiluminescence the transient location of the flame front can be monitored by the evaporation of oil droplets in areas of elevated temperatures. The chemically inert MgO particles were replaced by oil droplets. The Mie scattering of the droplets in the cold gas can be used simultaneously to process the instantaneous two-component velocity field. In the following example, double pulses from the Nd:YVO_4 laser with a pulse-to-pulse separation of 50 µs were generated at an overall repetition rate of 2.5 kHz. The CMOS camera was operated without IRO. The data post-processing was based on a PIV-algorithm presented in [15]. Interrogation areas of 16 x 16 pixels corresponded to 400 x 400 μm^2 in the measurement plane. The top of figure 7 shows one individual velocity map out of a sequence consisting of up to 4500 acquisitions.

The aim of this experiment was to track the temporal development of eddies approaching the flame front causing flame extinction. For this purpose a proper orthogonal decomposition (POD) of the considered data set was conducted [16]. POD provides an optimal set of basis functions for the selected ensemble of data. For each velocity map time-dependent coefficients were extracted resulting in an amplitude spectrum. This spectrum was band-pass filtered. A band-pass filter was chosen such that mean velocity, large-scale shear as well as small scale structures were subtracted. Finally, in a back-transformation a velocity map was reconstructed that carried mainly the information of the most-energetic vortices. The lower part of figure 7 shows a temporal sequence of filtered velocity maps. In this example modes n,k =[3-10] in the amplitude spectrum were used. The first frame in this sequence corresponds to the unfiltered velocity map shown in the top of this figure. Obviously, POD filtering is a very effective scale decomposition which allows visualizing vortices.

In figure 7 the instantaneous flame position in the measurement plane is shown by white areas. The selected sequence shows the onset of flame extinction in a time-resolved manner. It can be observed that the flame is thinned over a period of few ms. This thinning is a consequence of a counter-rotating pair of vortices located on the fuel side. During the extinction process the location of the counter-rotating vortices moved only marginally. In between the vortices a high local fluid flow is observed penetrating into the flame. Other realizations of extinction of this flame will be analyzed to extract final conclusions on the reasons for this process.

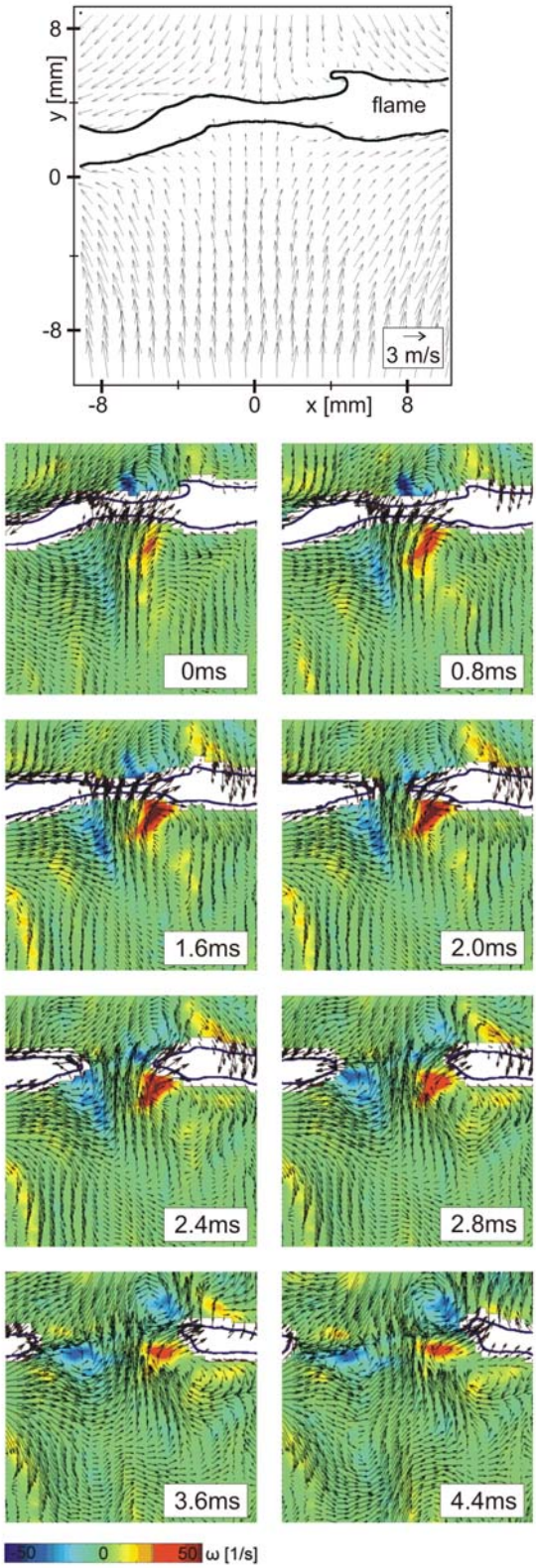

Figure 7: Instantaneous flow field prior to extinction (top), the location of the flame is represented by the white areas. PIV evaluation was possible only in the cold gases where the aerosol droplets have not yet evaporated. A time-resolved sequence of the filtered velocity field and the underlying vorticity field for an extinction event (bottom) Filtering was based on a POD.

Chemiluminescence at 10 kHz to observe flash back

Lean premixed combustion offers the potential for low NOx emissions. These flames, however, are hindered in their application as they are prone to instabilities and flash back. Therefore more knowledge is required to predict the transient behavior of such flames.

The burner presented at the right hand side of figure 1 was designed to investigate the transition from stable flames into flash back. Approaching a Reynolds-number dependent critical swirl number, the flame looms into the annular slot during precession. Figure 8 shows a sequence of chemiluminescence images during the event of a flash back. Tracking the temporal dynamics of the flame continuously is the only possibility to capture the point in time where flash back occurs. Thereby characteristics such as flame propagation speed can be measured conditioned on the transient event of flash back. Conventional repetition rates of several 10 Hz would be much too slow to capture the onset and dynamics of such an event.

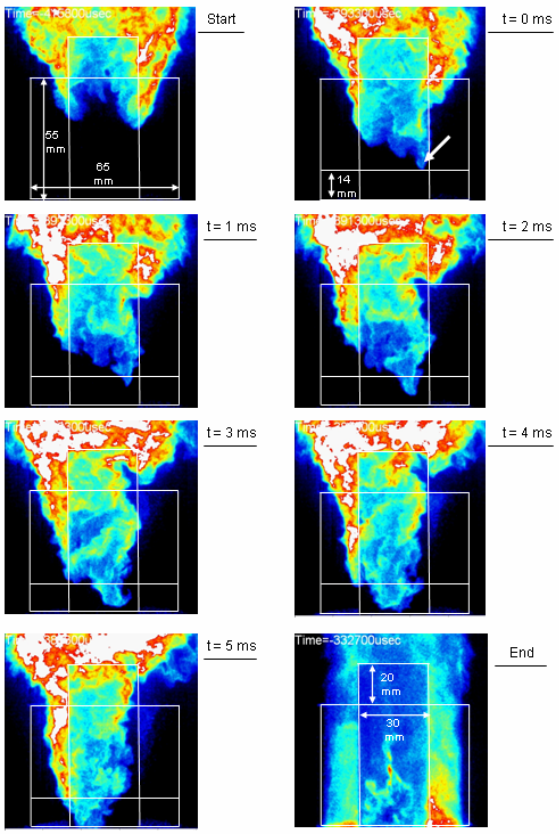

Figure 8: Sequence of CL images during flash back in the annular slot of the swirl burner. Although the IRO/CMOS data rate was 10 kHz only every 10th image is shown in the sequence labeled 0 to 5 ms. Finally the flame stabilizes at the swirler assembly inside the nozzle.

At the critical swirl number most of the times the flame extends into the slot. The arrow in the image at t=0 ms marks the instantaneous flame tip from which the flame shoots upstream subsequently. During this upstream movement the flame spins around the bluff body. Within 4 ms the flame covered a distance of 14 mm. This corresponds to an average axial velocity of 3.5 m/s. During other events the velocity peaked up to 12 m/s. The turbulent burning velocity is much less. For the present conditions it was estimated to be below 2 m/s according to [12]. As the kinematics of the premixed flame front can be determined by the vectorial addition of turbulent burning velocity and convection, the flash back must be caused by instantaneous negative axial gas velocities.

This conclusion needs additional evidence. In succeeding experiments instantaneous convection speeds need to be measured conditioned not only on the instant of flash back but simultaneously on the leading flame tip, too. This is required for "double-conditioning" and it seems to be feasible by planar diagnostics at high repetition rates.

OH PLIF at 5 kHz

In many previous studies relative OH distributions measured by planar laser-induced fluorescence (PLIF) served to identify the instantaneous location of the flame front. In contrast to Mie based methods, PLIF offers the potential of higher spatial resolution and reliability. Extending this method into the kHz-regime and combining it with PIV would certainly generate more insight into details of transient combustion processes such as flame front tracking.

In this study OH PLIF at a repetition rate of 5 kHz is reported. So far it was not combined with PIV. The tunable dye laser was pumped by the 90W Nd:YLF laser as described in the experimental section. The light sheet intersected the premixed turbulent flame at the center line. Here a swirl number of S=0 (compare left hand side of figure 3) was selected to prevent out-of-plane motions furthermost. Figure 9 shows the time-averaged chemiluminescence as monitored with the IRO/CMOS camera. The rectangle assigns the field of view of the OH PLIF measurements.

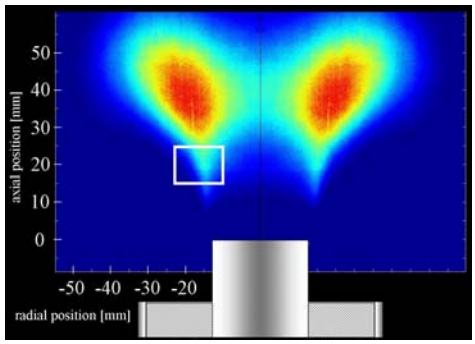

Figure 9: Time-averaged chemiluminescence of the unconfined premixed methane/air flame without swirl (S=0). The rectangle centered at (x;y)=(-16;+20)mm denotes the field of view of the 5 kHz OH PLIF measurements.

A subrange of 2ms from a ~1s long time sequence is shown in figure 10. The time lag between successive exposures was 200µs corresponding to 5 kHz. Obviously the repetition rate was high enough to obtain correlating images showing the flame front propagation from shot to shot. The flame front associated with the steep OH gradient can be extracted from this data.

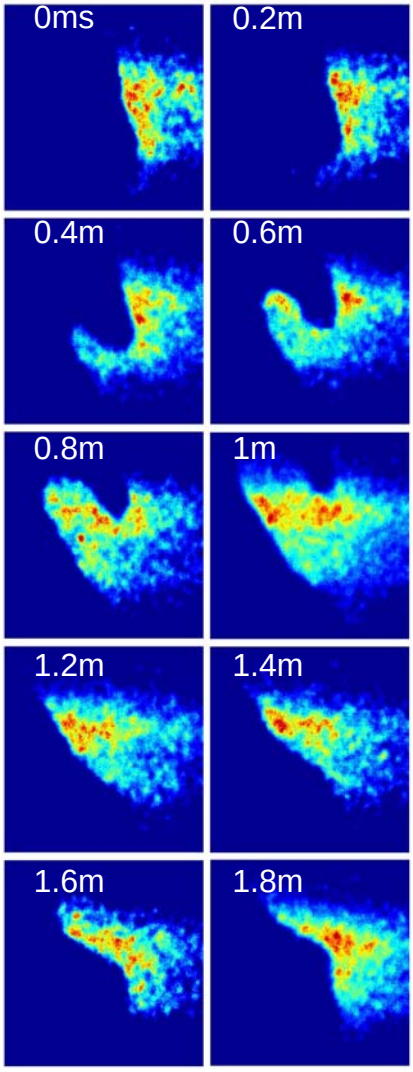

Figure 10: Sequence of 10 successive two-dimensional OH distributions measured with a repetition rate of 5 kHz in an unconfined premixed methane/air flame. The field of view is specified in figure 9.

Conclusions

This paper demonstrates the application of different optical diagnostic methods at repetition rates in the kHz-regime. For the selected examples the temporal resolution was short enough to resolve flow and flamedynamics at least of the larger scales. It was demonstrated that by rapid scanning of a measurement plane quasi-4D information can be gained. Furthermore transient events such as flash back, ignition or extinction can be tracked temporally over thousands of frames. Parts of the complete sequence can be selected to extract information on flow field or scalar properties of the flow at the occurrence of the transient event. This selection can be referred to as "conditioning on a transient event". These high-speed diagnostics complement the view on turbulent flames that have been investigated mainly by statistically independent sampling.

Acknowledgements

Financial support by Deutsche Forschungsgemeinschaft (DFG) through Sonderforschungsbereich 568, projects A4 and B1, Graduiertenkolleg 1344/1 and project DR 374/4-1 is kindly acknowledged.

References

[1] C.M. Fajardo, J. D. Smith, V. Sick, Appl. Phys. B 85 (2006) 25–30.
[2] A. Upatnieks, J.F. Driscoll, S. Ceccio, Proc. Combust. Inst. 29 (2002) 1897–1003.
[3] B. Wienecke, W. Reckers, 9th international Symposium on flow visualization (2000) 439-1 – 439-4.
[4] A. Winkler, J. Wäsle, T. Sattelmayer, Lasermethoden in der Strömungsmesstechnik 12 (2004) 18-1 – 18-8.
[5] J.D. Smith,V. Sick, Appl. Phys. B 81 (2005) 579–584.
[6] C. Kaminski, J. Hult, M. Aldén, S. Lindenmaier, A. Dreizler, U. Maas, M. Baum, Proc. Combust. Inst. 28 (2000) 399–405.
[7] S.F. Ahmed, E. Mastorakos, Combust. Flame 146 (2006) 215–231.
[8] T. Behrendt, M. Carl, C. Fleing, M. Frodermann, J. Heinze, C. Hassa, U. Meier, D. Wolff-Gaßmann, ASME 2000-GT-123.
[9] M. Raffel, C. Willert, J. Kompenhans, *Particle Image Velocimetry: a practical guide*, Berlin, Springer, 1998.
[10] D. Geyer, A. Kempf, A. Dreizler, J. Janicka, Proc. Combust. Inst. 30 (2005) 681–689.
[11] C. Schneider, A. Dreizler, J. Janicka, Flow Turbulence and Combustion 74 (2005) 103–127.
[12] A. Nauert, P. Petersson, M. Linne, A. Dreizler, 5th US Combustion Meeting, Paper E03, March 25-28 (2007).
[13] D. Geyer, A. Kempf, A. Dreizler, J. Janicka, Combust. Flame 143 (2005) 524–548.
[14] B. Delaunay: *Sur la sphere vide*. Bulletin of Academy of Sciences of the USSR (1934) 793–800.
[15] B. Böhm, D. Geyer, A. Dreizler, K.K. Venkatesan, N.M. Laurendeau, M.W. Renfro, Proc. Combust. Inst. 31 (2007) 709–717.
[16] R.J. Adrian, K.T. Christensen, Z.-C. Liu, Exp. in Fluids 29 (2000) 275–290.